

Synchronized flow in oversaturated city traffic

Boris S. Kerner,^{1,*} Sergey L. Klenov,² Gerhard Hermanns,¹ Peter Hemmerle,³ Hubert Rehborn,³ and Michael Schreckenberg¹

¹Physik von Transport und Verkehr, Universität Duisburg-Essen, 47048 Duisburg, Germany

²Department of Physics, Moscow Institute of Physics and Technology, 141700 Dolgoprudny, Moscow Region, Russia

³Daimler AG, GR/PT, HPC: G02I, 71059 Sindelfingen, Germany

(Received 24 August 2013; published 8 November 2013)

Based on numerical simulations with a stochastic three-phase traffic flow model, we reveal that moving queues (moving jams) in oversaturated city traffic dissolve at some distance upstream of the traffic signal while transforming into synchronized flow. It is found that, as in highway traffic [Kerner, *Phys. Rev. E* **85**, 036110 (2012)], such a jam-absorption effect in city traffic is explained by a strong driver's speed adaptation: Time headways (space gaps) between vehicles increase upstream of a moving queue (moving jam), resulting in moving queue dissolution. It turns out that at given traffic signal parameters, the stronger the speed adaptation effect, the shorter the mean distance between the signal location and the road location at which moving queues dissolve fully and oversaturated traffic consists of synchronized flow only. A comparison of the synchronized flow in city traffic found in this Brief Report with synchronized flow in highway traffic is made.

DOI: [10.1103/PhysRevE.88.054801](https://doi.org/10.1103/PhysRevE.88.054801)

PACS number(s): 89.40.-a, 47.54.-r, 64.60.Cn, 05.65.+b

There are two main types of city traffic at traffic signals: under- and oversaturated traffic. In undersaturated traffic, all vehicles which are waiting within a queue during the red phase can pass the signal during the green phase. The opposite case occurs in oversaturated traffic: some of the vehicles in the queue cannot pass the signal location during the green phase, resulting in queue growth [Figs. 1(a) and 1(b)] [1]. In accordance with the classical theory [1], well-developed oversaturated traffic consists of a sequence of moving queues, with stopped vehicles separated by regions in which vehicles move from one moving queue to the adjacent downstream moving queue; the mean duration of the vehicle stop within a moving queue does not usually change while the moving queue propagates upstream of the signal [Fig. 1(c)].

It is usually assumed [1] that the transition from under- to oversaturated traffic, i.e., traffic breakdown at the signal occurs at a classical capacity of traffic signal $C_{cl} = q_{sat} T_G^{(eff)} / \vartheta$, where q_{sat} is the saturation flow rate, i.e., the mean flow rate from a queue at the signal during the green phase when vehicles discharge from the moving queue to their maximum free speed v_{free} ; $\vartheta = T_G + T_Y + T_R$ is the cycle time of the signal assumed to be constant; T_G , T_Y , and T_R are the durations of the green, yellow, and red phases of the signal, respectively; $T_G^{(eff)}$ is the effective green-phase time, which is the portion of the cycle time during which vehicles are assumed to pass the signal at a constant rate q_{sat} [1].

In contrast with this assumption of the classical theories, as found in [2], with some probability undersaturated traffic exists for a long time interval, even if the average arrival flow rate \bar{q}_{in} exceeds the classical capacity. This is true as long as $\bar{q}_{in} < C_{max}$, where C_{max} is the maximum capacity of the signal, which is larger than C_{cl} . In this three-phase theory of *undersaturated city traffic*, a crucial role for traffic breakdown is the occurrence of synchronized flow in the neighborhood of the signal [2,3].

In this Brief Report we find out that synchronized flow can also occur in *oversaturated city traffic* and reveal the physics of this effect. We apply results of [4], in which a jam-absorption effect in highway traffic is studied: When a driver's speed adaptation to the speed of the preceding vehicle is strong enough, time headways (space gaps) between vehicles increase considerably upstream of a moving jam, resulting in jam dissolution. In contrast with two-phase traffic flow models with a fundamental diagram (e.g., [5–7]), in a stochastic model [8] used for all simulations, this speed adaptation occurs within a two-dimensional (2D) region of synchronized flow associated with the fundamental hypothesis of three-phase theory (Fig. 2) [9]. When a driver approaches a slower-moving preceding vehicle but cannot overtake it, the driver begins to decelerate and adapts his or her speed to the speed of the preceding vehicle when the gap g to the preceding vehicle becomes smaller than a synchronization gap G [Fig. 2(b)]. This driver's speed adaptation occurs under the condition $g_{safe} \leq g \leq G$, where g_{safe} is a safe gap. The stronger the speed adaptation, the larger is the mean space gap (the longer the mean time headway) between vehicles in synchronized flow.

We use a discrete version of a stochastic three-phase microscopic model of Kerner and Klenov [8]. The physics of model variables has been explained in [9] and in more detail in the Supplemental Material [10]. In the model whose parameters have been adapted for city traffic in [2], the vehicle speed v_{n+1} , coordinate x_{n+1} , and acceleration A_{n+1} at time step $n + 1$ are found from the equations

$$v_{n+1} = \max(0, \min(v_{free}, \tilde{v}_{n+1} + \xi_n, v_n + a_{max} \tau, v_{s,n})), \quad (1)$$

$$x_{n+1} = x_n + v_{n+1} \tau, \quad (2)$$

$$A_{n+1} = (v_{n+1} - v_n) / \tau, \quad (3)$$

$$\tilde{v}_{n+1} = \min(v_{free}, v_{s,n}, v_{c,n}), \quad (4)$$

$$v_{c,n} = \begin{cases} v_{c,n}^{(1)} & \text{at } \Delta v_n + A_{\ell,n} \tau < \Delta v_a, \\ v_{c,n}^{(2)} & \text{at } \Delta v_n + A_{\ell,n} \tau \geq \Delta v_a, \end{cases} \quad (5)$$

*boris.kerner@uni-due.de

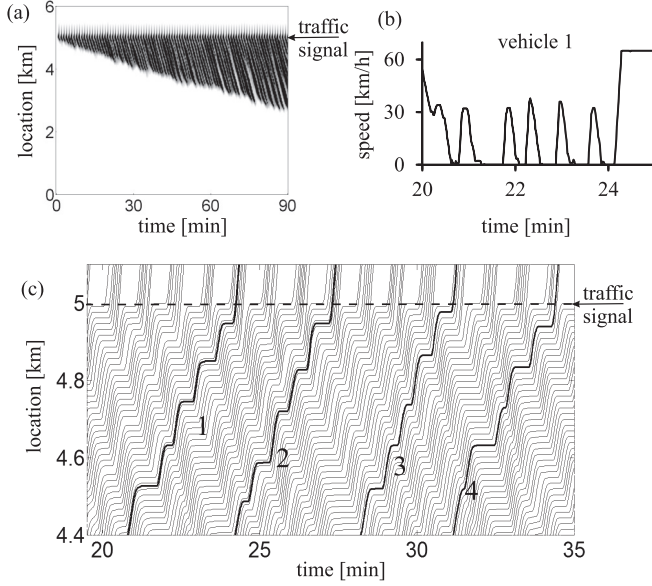


FIG. 1. Spatiotemporal structure of oversaturated traffic at a traffic signal of the classical theory of city traffic [1] simulated with the model (1)–(21): (a), (b) Speed in space and time represented by regions with variable shades of gray (a) (in white regions the speed is higher than 50 km/h; in black regions the speed is 0) and microscopic (single-vehicle) speed along vehicle trajectory 1 (b) shown in (c). (c) Vehicle trajectories for some time interval and for a 600-m-long road section upstream of the signal location at $x = 5$ km from the beginning ($x = 0$) of a single-lane road (each second trajectory is shown); vehicle trajectories 1–4 illustrate the spatiotemporal structure of oversaturated traffic. Signal parameters: $\vartheta = 60$ s, $T_R = 28$ s, $T_Y = 2$ s. The arrival flow rate is time independent: $q_{in} = 1000$ vehicles/h. The saturation flow rate $q_{sat} = 1880$ vehicles/h. The classical capacity $C_{cl} = 902$ vehicles/h. Model parameters are $\tau_{safe} = \tau = 1$, $d = 7.5$ m, $v_{free} = 18.0558$ ms $^{-1}$ (65 km/h), $b = 1$ ms $^{-2}$, $a = 0.5$ ms $^{-2}$, $k = 3$, $\phi_0 = 1$, $\Delta v_a = 2$ ms $^{-1}$, $k_a = 4$, $\gamma = 1$, $p_b = 0.1$, $p_a = 0.03$, $\varepsilon = 0$, $p^{(0)} = 0.005$, $p_0(v_n) = 0.667 + 0.083 \min(1, v_n/v_{01})$, $v_{01} = 6$ ms $^{-1}$, $v_{21} = 7$ ms $^{-1}$. $a^{(a)} = a$, $a^{(0)} = 0.2a$, $a^{(b)}(v_n) = 0.2a + 0.8a \max(0, \min(1, (v_{22} - v_n)/\Delta v_{22}))$, $v_{22} = 7$ ms $^{-1}$, $\Delta v_{22} = 2$ ms $^{-1}$.

Δv_a is constant,

$$v_{c,n}^{(1)} = \begin{cases} v_n + \Delta_n^{(1)} & \text{at } g_n \leq G_n, \\ v_n + a_n \tau & \text{at } g_n > G_n, \end{cases} \quad (6)$$

$$\Delta_n^{(1)} = \max(-b_n \tau, \min(a_n \tau, v_{\ell,n} - v_n)), \quad (7)$$

$$v_{c,n}^{(2)} = v_n + \Delta_n^{(2)}, \quad (8)$$

$$\Delta_n^{(2)} = k_a a_n \tau \max(0, \min(1, \gamma(g_n - v_n \tau))), \quad (9)$$

$$a_{max} = \begin{cases} a & \text{at } \Delta v_n + A_{\ell,n} \tau < \Delta v_a, \\ k_a a & \text{at } \Delta v_n + A_{\ell,n} \tau \geq \Delta v_a, \end{cases} \quad (10)$$

$$a_n = a \Theta(P_0 - r_1), \quad b_n = a \Theta(P_1 - r_1), \quad (11)$$

$$P_0 = \begin{cases} p_0 & \text{if } S_n \neq 1, \\ 1 & \text{if } S_n = 1, \end{cases} \quad P_1 = \begin{cases} p_1 & \text{if } S_n \neq -1, \\ p_2 & \text{if } S_n = -1, \end{cases} \quad (12)$$

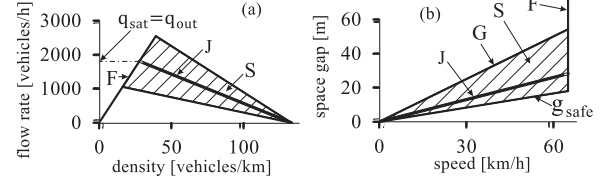


FIG. 2. Two-dimensional regions for steady states of synchronized flow in (a) the flow-density and (b) the space-gap-speed planes [2,8]. F, free flow; S, synchronized flow; J, line J [9].

$$S_{n+1} = \begin{cases} -1 & \text{if } \tilde{v}_{n+1} < v_n, \\ 1 & \text{if } \tilde{v}_{n+1} > v_n, \\ 0 & \text{if } \tilde{v}_{n+1} = v_n, \end{cases} \quad (13)$$

$r_1 = \text{rand}(0, 1)$, $\Theta(z) = 0$ at $z < 0$ and $\Theta(z) = 1$ at $z \geq 0$, $p_0 = p_0(v_n)$, $p_2 = p_2(v_n)$, p_1 is constant,

$$\xi_n = \begin{cases} \xi_a & \text{if } S_{n+1} = 1, \\ -\xi_b & \text{if } S_{n+1} = -1, \\ \xi^{(0)} & \text{if } S_{n+1} = 0, \end{cases} \quad (14)$$

$$\xi_a = a^{(a)} \tau \Theta(p_a - r), \quad \xi_b = a^{(b)} \tau \Theta(p_b - r), \quad (15)$$

$$\xi^{(0)} = a^{(0)} \tau \begin{cases} -1 & \text{if } r \leq p^{(0)}, \\ 1 & \text{if } p^{(0)} < r \leq 2p^{(0)} \text{ and } v_n > 0, \\ 0 & \text{otherwise,} \end{cases} \quad (16)$$

$r = \text{rand}(0, 1)$; $a^{(b)} = a^{(b)}(v_n)$; p_a , p_b , $p^{(0)}$, $a^{(a)}$, and $a^{(0)}$ are constants; synchronization gap G_n and safe speed $v_{s,n}$ are

$$G_n = G(v_n, v_{\ell,n}), \quad (17)$$

$$G(u, w) = \max(0, \lfloor k \tau u + a^{-1} \phi_0 u(u - w) \rfloor), \quad (18)$$

$$v_{s,n} = \min(v_n^{(safe)}, g_n/\tau + v_{\ell}^{(a)}), \quad (19)$$

$$v_n^{(safe)} = \lfloor v^{(safe)}(g_n, v_{\ell,n}) \rfloor, \quad (20)$$

$v^{(safe)} \tau_{safe} + X_d(v^{(safe)}) = g_n + X_d(v_{\ell,n})$, $X_d(u) = b \tau^2 (\alpha \beta + \frac{\alpha(\alpha-1)}{2})$, $\alpha = \lfloor u/b \tau \rfloor$, $\beta = u/b \tau - \alpha$, $v_{\ell}^{(a)} = \max(0, \min(v_{\ell,n}^{(safe)}, v_{\ell,n}, g_{\ell,n}/\tau) - a \tau)$, τ_{safe} is a safe time gap; b , $k > 1$, a , k_a , and ϕ_0 are constants; and $\lfloor z \rfloor$ denotes the integer part of a real number z . In (1)–(20), $n = 0, 1, 2, \dots$ is the number of time steps, $\tau = 1$ s is a time step, a_{max} is a maximum acceleration, v_{free} is a maximum speed in free flow, \tilde{v}_n is the vehicle speed without speed fluctuations ξ_n , ℓ marks the preceding vehicle, $g_n = x_{\ell,n} - x_n - d$ is the space gap between vehicles, d is the vehicle length, $\Delta v_n = v_{\ell,n} - v_n$; x_n and v_n are measured in units of δx and δv , respectively, where $\delta x = 0.01$ m and $\delta v = 0.01$ m/s. In the model, vehicles decelerate at the upstream front of a moving queue at a signal as they do at the upstream front of a wide moving jam propagating on a road without traffic signals [9]. During the green phase, vehicles accelerate at the downstream front of the moving queue (queue discharge) with a random time delay as they do at the downstream jam front; in other words, the well-known saturation flow rate of a moving queue discharge is equal to the jam outflow q_{out} under the condition that vehicles accelerate to the maximum speed v_{free} , i.e., in

this case $q_{\text{sat}} = q_{\text{out}}$ [Fig. 2(a)]. During the yellow phase the vehicle passes the signal location, if the vehicle can do it until the end of the yellow phase; otherwise, the vehicle comes to a stop at the signal. As in studies of other physical features of city traffic (e.g., [11]), it is sufficient to consider traffic at a *single* city intersection. Open boundary conditions have been used in all simulations.

We use a stochastic description of driver speed adaptation through probabilities p_2 and p_1 in (12). Introducing a coefficient of speed adaptation ε , we write these probabilities as

$$p_1 = \min(1, (1 + \varepsilon)p_1^{(0)}), \quad p_2 = \min(1, (1 + \varepsilon)p_2^{(0)}(v_n)), \quad (21)$$

where $p_1^{(0)} = 0.3$ and $p_2^{(0)}(v_n) = 0.48 + 0.32\Theta(v_n - v_{21})$. We have found that the larger is ε , the stronger the speed adaptation in the 2D region of synchronized flow and, therefore, the larger the mean space gap (the longer the mean time headway) between vehicles in synchronized flow.

Under “usual” speed adaptation ($\varepsilon = 0$), the mean duration of the vehicle stop within a moving queue does not change while the moving queue moves away from the signal; therefore, the vehicle speed exhibits a usual sequence of the stops within moving queues and vehicle motion (acceleration with the subsequent deceleration) between the moving queues [Figs. 1(b) and 1(c)]. In contrast, when ε increases, the mean duration of the vehicle stop within a moving queue decreases when the moving queue moves farther and farther away from the signal location. As a result, when the moving queues are far enough upstream from the signal location some of them dissolve fully and transform into synchronized flow [Figs. 3(a)–3(c)].

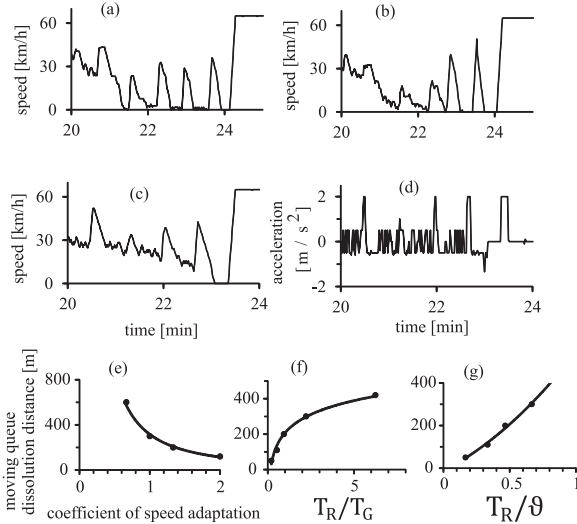


FIG. 3. Simulations of characteristics of moving queue dissolution and synchronized flow occurrence: (a–d) Microscopic (single-vehicle) speeds (a–c) and vehicle acceleration (d) along some vehicle trajectories at $\varepsilon = 0.667$ (a), $\varepsilon = 1.0$ (b), and $\varepsilon = 2.0$ (c, d). (e–g) Mean distance between the signal location and the road location at which moving queues dissolve (“moving queue dissolution distance”) as functions of the coefficient of speed adaptation ε (e), T_R/T_G (f), and T_R/θ (g). In (f) and (g), $\varepsilon = 1.333$. Other parameters are the same as in Fig. 1.

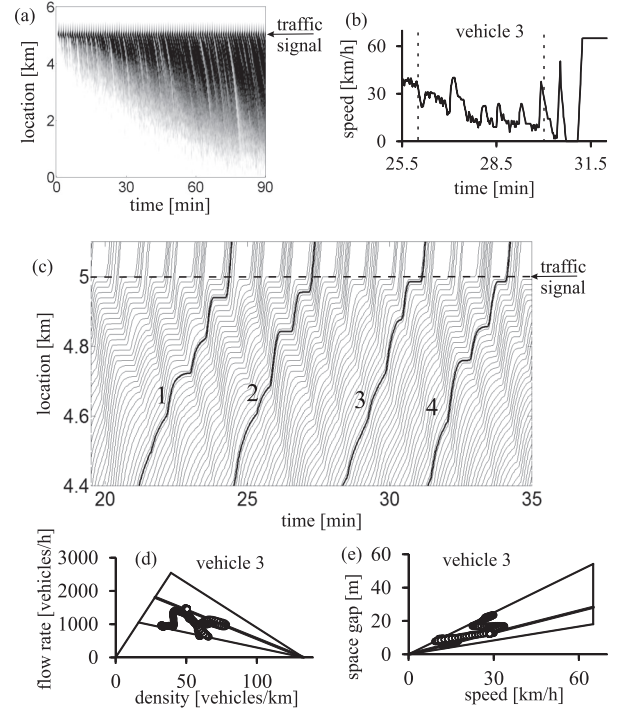


FIG. 4. Simulations of the spatiotemporal effect of moving queue dissolution with synchronized flow occurrence under strong speed adaptation at $\varepsilon = 1.333$ ($p_1 = 0.7$, $p_2 = 1$): (a, b) Speed in space and time represented by regions with variable shades of gray (a) and microscopic speed along vehicle trajectory 3 (b) shown in (c). (c) Fragment of vehicle trajectories upstream of the signal (each second trajectory is shown); vehicle trajectories 1–4 illustrate the spatiotemporal structure of oversaturated traffic. (d, e) Synchronized flow along trajectory 3 in (c) [20-s moving average of data within the time interval labeled by vertical dotted lines in (b)] shown within 2D regions for steady states of synchronized flow in the flow density (d) and the space-gap–speed (e) planes taken from Fig. 2. Other parameters are the same as those in Fig. 1.

A *general behavior* of oversaturated city traffic under stronger speed adaptation is as follows: (i) The mean duration of a vehicle stop within a moving queue decreases while the moving queue moves away upstream from the signal [Figs. 3(a) and 3(b)]. (ii) At some distance of the signal location [called the “moving queue dissolution distance” in Figs. 3(e)–3(g)], moving queues dissolve and oversaturated traffic consists of synchronized flow only, in which vehicles do not come to a stop at all [Figs. 4(b) and 4(c)]. (iii) The stronger the speed adaptation (the larger the value of ε), the shorter the moving queue dissolution distance [Fig. 3(e)]. (iv) The moving queue dissolution distance is shorter the lower the ratios T_R/T_G and T_R/θ [Figs. 3(f) and 3(g)]. (v) At strong enough speed adaptation, vehicles stop only a few (one or two) times in the neighborhood of the signal location [Figs. 3(c), 4(b), and 4(c)]. This means that all moving queues dissolve and transform into synchronized flow already at relatively short distances upstream of the signal location. In this case, in contrast with the classical theory [Figs. 1(b) and 1(c)], a vehicle accelerates and decelerates many times during its movement in synchronized flow [Fig. 3(d)]. (vi) The upstream front of this

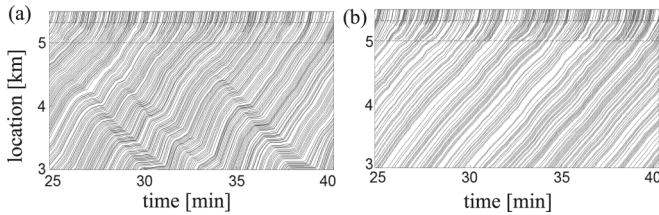


FIG. 5. Simulations of the transformation of a general pattern (GP) at on-ramp bottleneck in highway traffic into a widening synchronized flow pattern (WSP) under increase in speed adaptation: (a, b) Fragments of vehicle trajectories within the GP calculated at $\varepsilon = 0$ (a) and within the WSP calculated at $\varepsilon = 1.333$ (b) (each second trajectory is shown). $q_{\text{in}} = 2000$ and $q_{\text{on}} = 1200$ vehicles/h, $v_{\text{free}} = 108$ km/h, on-ramp location $x_{\text{on}} = 5$ km. The model of the on-ramp is taken from [9]. $p_0(v_n) = 0.575 + 0.125 \min(1, v_n/v_{01})$, $v_{01} = 10 \text{ ms}^{-1}$, $v_{21} = 15 \text{ ms}^{-1}$, $v_{22} = 12.5 \text{ ms}^{-1}$, $\Delta v_{22} = 2.78 \text{ ms}^{-1}$. Other parameters of the model, (1)–(21), are the same as in Fig. 1.

synchronized flow propagates more quickly [Fig. 4(a)] than in the well-known classical case shown in Fig. 1(a).

The physics of moving queue dissolution (moving queue absorption) in oversaturated city traffic is as follows. For a strong enough driver speed adaptation, synchronized flow states lie mostly on and below the line J in the flow-density plane and, respectively, on and above the line J in the space-gap-speed plane [circles in Figs. 4(d) and 4(e)]. In this synchronized flow no moving queues can persist over time [4,9]. This is because the mean space gap between vehicles

under strong speed adaptation is large. Therefore, space gaps (time headways) between vehicles increase considerably upstream of moving queues. As a result, the absolute value of the upstream front velocity of a moving queue becomes smaller than that of the downstream front of the moving queue, resulting in moving queue dissolution.

A qualitative difference between synchronized flow occurrence in oversaturated city traffic revealed here [Figs. 4(a)–4(c)] and the jam-absorption effect leading to the transformation of a general pattern [Fig. 5(a)] into a widening synchronized flow pattern at an on-ramp bottleneck [Fig. 5(b)] [4] is as follows: At the on-ramp bottleneck there is usually noninterrupted flow. Therefore, no wide moving jams should necessarily occur at the highway bottleneck. In contrast, in city traffic vehicles must stop at the signal during the red phase. Therefore, there is usually a queue with stopped vehicles at the signal regardless of how strong speed adaptation is. However, with a strong enough speed adaptation this queue dissolves quickly while moving away from the signal location transforming into synchronized flow. For an empirical verification of the model predictions, measurements of spatiotemporal speed distribution in oversaturated city traffic are required. We plan to do such measurements in the near-future.

We thank our partners for their support in the project UR:BAN—Urban Space: User Oriented Assistance Systems and Network Management, funded by the German Federal Ministry of Economics and Technology by resolution of the German Federal Parliament.

-
- [1] F. V. Webster, Road Research Technical Paper No. 39 (Road Research Laboratory, London, 1958); G. F. Newell, *SIAM Rev.* **575**, 223 (1965); J. D. C. Little, *Operat. Res.* **14**, 568 (1966); D. I. Robertson, TRRL Report No. LR 253 (Transport. Road Res. Lab., Crow Thorne, UK, 1969); N. H. Gartner and Ch. Stamatiadis, in *Encyclopedia of Complexity and System Science*, edited by R. A. Meyers (Springer, Berlin, 2009), pp. 9470–9500; F. Dion, H. Rakha, and Y. S. Kang, *Transport. Res. B* **38**, 99 (2004).
 - [2] B. S. Kerner, arXiv:1211.2535v1; *Europhys. Lett.* **102**, 28010 (2013).
 - [3] B. S. Kerner, *Phys. Rev. E* **84**, 045102(R) (2011).
 - [4] B. S. Kerner, *Phys. Rev. E* **85**, 036110 (2012).
 - [5] P. G. Gipps, *Transport. Res. B* **15**, 105 (1981).
 - [6] K. Nagel and M. Schreckenberg, *J. Phys. (France) I* **2**, 2221 (1992); R. Barlović, L. Santen, A. Schadschneider, and M. Schreckenberg, *Eur. Phys. J. B* **5**, 793 (1998).
 - [7] S. Krauß, P. Wagner, and C. Gawron, *Phys. Rev. E* **55**, 5597 (1997).
 - [8] B. S. Kerner and S. L. Klenov, *J. Phys. A: Math. Gen.* **35**, L31 (2002); *Phys. Rev. E* **68**, 036130 (2003); **80**, 056101 (2009).
 - [9] B. S. Kerner, *The Physics of Traffic* (Springer, Berlin, 2004); *Introduction to Modern Traffic Flow Theory and Control* (Springer, Berlin, 2009).
 - [10] See Supplemental Material at <http://link.aps.org/supplemental/10.1103/PhysRevE.88.054801> for model details.
 - [11] E. Brockfeld, R. Barlovic, A. Schadschneider, and M. Schreckenberg, *Phys. Rev. E* **64**, 056132 (2001).